Pulmonary artery smooth muscle cell pyroptosis promotes the proliferation of PASMCs by paracrine IL-1β and IL-18 in monocrotaline-induced pulmonary arterial hypertensive rats

QIN-YI ZHOU[1,2*], WANG LIU[1,2*], SHAO-XIN GONG[3], YING TIAN[4], XIAO-FENG MA[1,2] and AI-PING WANG[2,4]

[1]Department of Cardiology, Affiliated Nanhua Hospital, Hengyang Medical School, University of South China, Hengyang, Hunan 421002, P.R. China; [2]Institute of Clinical Research, Affiliated Nanhua Hospital, Hengyang Medical School, University of South China, Hengyang, Hunan 421001, P.R. China; [3]Department of Pathology, First Affiliated Hospital, Hengyang Medical School, University of South China, Hengyang, Hunan 421001, P.R. China; [4]Department of Physiology, Institute of Neuroscience Research, Hengyang Medical School, University of South China, Hengyang, Hunan 421001, P.R. China

Received January 26, 2024; Accepted July 12, 2024

DOI: 10.3892/etm.2024.12683

Abstract. Pulmonary arterial hypertension (PAH) is a common vascular disease, and pulmonary vascular remodeling is a pivotal pathophysiological mechanism of PAH. Major pathological changes of pulmonary arterial remodeling, including proliferation, hypertrophy and enhanced secretory activity, can occur in pulmonary artery smooth muscle cells (PASMCs). Multiple active factors and cytokines play important roles in PAH. However, the regulatory mechanisms of the active factors and cytokines in PAH remain unclear. The present study aimed to reveal the crucial role of PASMC pyroptosis in PAH and to elucidate the intrinsic mechanisms. To establish the PAH rat models, Sprague-Dawley rats were injected intraperitoneally with monocrotaline (MCT) at a dose of 60 mg/kg. The expression of proteins and interleukins were detected by western blotting and ELISA assay. The results indicated that the pyroptosis of PASMCs is significantly increased in MCT-induced PAH rats. Notably, pyroptotic PASMCs can secret IL-1β and IL-18 to promote the proliferation of PASMCs. On this basis, inhibiting the secretion of IL-1β and IL-18 can markedly inhibit PASMC proliferation. Collectively, the findings of the present study indicate a critical role for PASMC pyroptosis in MCT-induced PAH rats, prompting a new preventive and therapeutic strategy for PAH.

Correspondence to: Professor Xiao-Feng Ma, Department of Cardiology, Affiliated Nanhua Hospital, Hengyang Medical School, University of South China, 336 South Dongfeng Road, Hengyang, Hunan 421002, P.R. China
E-mail: mxf13786437543@163.com

Professor Ai-Ping Wang, Department of Physiology, Institute of Neuroscience Research, Hengyang Medical School, University of South China, 28 West Changsheng Road, Hengyang, Hunan 421001, P.R. China
E-mail: waiping2011@163.com; waiping2011@usc.edu.cn

*Contributed equally

Abbreviations: GSDMD, gasdermin D; HE, hematoxylin-eosin; IL-1β, interleukin 1β; IL-18, interleukin 18; LV, left ventricle; MCT, monocrotaline; mPAP, mean pulmonary artery pressure; NLRP3, Nod-like receptor protein 3; PAH, pulmonary arterial hypertension; PASMCs, pulmonary artery smooth muscle cells; PCNA, proliferating cell nuclear antigen; RV, right ventricle; RVSP, right ventricular systolic pressure; S, interventricular septum; SD, Sprague-Dawley; SMCs, smooth muscle cells; VSMCs, vascular smooth muscle cells; WT, pulmonary artery wall thickness

Key words: pulmonary artery smooth muscle cells, pyroptosis, gasdermin D, interleukin 1β, interleukin 18, pulmonary arterial hypertension

Introduction

Pulmonary arterial hypertension (PAH) is a refractory cardiovascular disease accompanied by varying degrees of inflammation, which currently lacks a curative treatment method (1). The major pathological features of PAH are pulmonary vascular remodeling and progressive obstruction, leading to increased pulmonary artery pressure, and ultimately severe heart failure and death (2). Previous research has shown that the 10-year survival rate of patients is only 45-66% (3). Although there are various drugs that can alleviate the clinical symptoms of patients with PAH to a certain extent, the mortality rate remains high, and death from failure of the right ventricle occurs in ~40% of patients within 5 years of diagnosis (4,5). However, the specific pathogenesis of PAH has not been fully elucidated (6,7). Therefore, there is an urgent need to explore the pathogenesis of PAH and identify effective targets for its diagnosis and treatment.

Pulmonary vascular remodeling is a key pathophysiological mechanism in PAH progression and is often accompanied by pathological changes such as injury and migration of vascular endothelial cells, thickening of the pulmonary artery media [mainly pulmonary artery smooth muscle cells (PASMCs)], and pathological deposition of the extracellular

matrix (8). Pulmonary arterioles (diameter, <100 μm) are key remodeling vessels during PAH (9). Importantly, PASMC proliferation and hypertrophy are considered significant pathological characteristics of pulmonary vascular remodeling in PAH (10,11). An increasing number of studies have revealed that senescence, apoptosis and pyroptosis of PASMCs may participate in PAH progression, and are accompanied by changes in various cytokines and inflammatory factors (such as IL-1β and IL-6) that regulate the proliferation and phenotypic transformation of PASMCs (12-14). However, the mechanisms that regulate inflammatory factors to promote PASMC proliferation in PAH remain unclear. Therefore, identifying a novel pathophysiological mechanism that inhibits PASMC proliferation is important for the prevention and treatment of PAH.

Pyroptosis is a specialized form of programmed cell death accompanied by a pro-inflammatory response (15). Nod-like receptor protein 3 (NLRP3) is a typical pyroptotic protein. The NLRP3 inflammasome, a cytosolic protein complex for early inflammatory responses, is composed of apoptosis-associated speck-like protein containing a caspase recruitment domain, NLRP3 and Caspase-1 (16). After NLRP3 is activated, pro-caspase-1 is cleaved into activated Caspase-1 (17). After the activation of cysteine protease by NLRP3, the activation and self-digestion of Caspase-1 leads to the cleavage of the substrate gasdermin D (GSDMD). GSDMD initiates the formation of membrane pores. Several pores are formed on the membrane, allowing inflammatory factors (such as IL-1β and IL-18) to be cleaved into mature forms (18). Subsequently, pyroptotic cells swell, and the cell membrane ruptures, further promoting inflammatory factor release, activating a strong inflammatory stress response, and eventually accelerating the development and progression of PAH (19). Previous studies have demonstrated that inhibiting pyroptosis in vascular smooth muscle cells (VSMCs) is crucial for preventing the occurrence and progression of vascular diseases. Xu *et al (*20) confirmed that VSMC pyroptosis accelerates atherosclerotic plaque formation and aggravates plaque instability (20). In addition, when a high-fat diet is used *in vivo* in an animal study or the VSMCs are treated with oxidized low-density lipoprotein *in vitro*, VSMC pyroptosis promotes abnormal proliferation and migration of VSMCs, leading to the progression of arteriosclerosis (21,22). Studies have confirmed that VSMC pyroptosis is involved in pathological processes such as acute lung injury, atherosclerosis and vascular remodeling (23-25). These studies suggest that VSMC pyroptosis plays a significant role in cardiovascular disease. However, the pivotal role and mechanism of VSMC pyroptosis in rats with monocrotaline (MCT)-induced PAH remains unclear. MCT is a macrocyclic pyrrolizidine alkaloid that causes a pulmonary vascular syndrome in rats characterized by pulmonary hypertension (26). The GSDM protein family oligomerizes to form large pores in the membrane that drive swelling and membrane rupture (27), with various researchers defining pyroptosis as a form of GSDMD-mediated programmed cell death (28,29). In our preliminary experiments, it was found that GSDMD protein expression was significantly upregulated *in vivo*. Hence, it was hypothesized that PASMC pyroptosis may be a novel pathophysiological mechanism for promoting PAH, and its molecular mechanisms may be related to the formation of GSDMD membrane pores and the secretion of interleukins in MCT-induced PAH rats.

In the present study, PAH rats were treated with MCT. The aim of this study was to demonstrate the role of pyroptosis in pulmonary hypertension. With regard to the mechanism, this study would show whether pyroptotic PASMCs promote PASMC proliferation by secreting IL-1β and IL-18 in MCT-induced PAH. The present study provides new insights into the pathophysiological mechanisms of PAH, as well as a new direction for developing a targeted and novel therapeutic option against PAH.

Materials and methods

Animals. Male Sprague-Dawley (SD) rats, aged 6-8 weeks, weighing 185-205 g, were purchased from Hunan Silaike Jingda Laboratory Animal Co., Ltd. and housed at the Laboratory Animal Center of Hengyang Medical School (University of South China; Hengyang, China). Rats were labelled and allowed to drink freely. The ambient temperature was set to 18-22˚C and the humidity was 50-60%, with a 12-h light and 12-h darkness cycle. All experiments were performed in strict accordance with the ARRIVE guidelines and approved by The Animal Ethics Committee of the University of South China (Hengyang, China; approval no. 446).

Animal experiments. A total of 30 male SD rats were acclimatized for one week. After which, the rats were randomly divided into three groups (n=10/group) including: i) Control group; ii) vehicle group; and iii) MCT group. To establish the PAH rat models, SD rats in the MCT group were injected intraperitoneally with MCT (cat. no. C2401; Millipore Sigma) at a dose of 60 mg/kg. The rats in the vehicle group were intraperitoneally injected with the same volume of the vehicle (10% DMSO + 40% PEG400 + 50% saline), while the rats in the control group were not treated.

A total of 40 male SD rats were acclimatized for one week. The second batch of rats were randomly divided into four groups (n=10/group) including: i) Control group; ii) vehicle group; iii) MCT group; and iv) disulfiram-treated PAH group (MCT + disulfiram group). The rats in the MCT + disulfiram group were treated with disulfiram (cat. no. HY-B0240; MedChem Express) injected intraperitoneally at a dose of 20 mg/kg, 24 h before MCT treatment and 5, 10, 15 and 20 days after MCT treatment (the same dose of MCT was used for these rats). Simultaneously, vehicle rats were intraperitoneally injected with the same volume of the vehicle. The MCT-induced and the control rats were treated in the same manner as aforementioned.

The rats were weighed separately over seven days and fed a normal diet. Rats were monitored closely for any severe impairment in physiological or neurological function and were euthanized when these signs became apparent. Each rat was anesthetized via intraperitoneal injection with pentobarbital (40 mg/kg), and the right ventricular systolic pressure (RVSP) and mean pulmonary arterial pressure (mPAP) were measured through the jugular vein using a transvenous catheter, as previously described (30). Subsequently, a total of 1.5 ml blood was collected from the right ventricle and placed in a tube to determine the serum level of IL-1β and IL-18, and the

rats were sacrificed by exsanguination via the jugular vein and carotid artery. Animal death was confirmed by the cessation of heart rate and a lack of breathing. The right ventricle (RV), left ventricle (LV) and interventricular septum (S) were isolated and weighed. The tibial length of the right leg was also monitored. The RV/(LV + S) and RV/tibial length ratios were assessed as they are considered essential for evaluating right ventricular hypertrophy. Finally, the pulmonary tissues were collected to detect differential protein expression.

Hematoxylin-eosin (HE) staining. Lung tissues were used to assess pathological alterations in pulmonary artery remodeling through HE staining. Pulmonary arteries were evaluated by an experienced pathologist and the isolated rat lung tissues were stained with HE to assess the degree of pulmonary vascular remodeling. The samples were fixed in 10% formalin for 12 h at 4˚C, and then embedded in paraffin for subsequent sectioning. The 5-μm specimens were first placed in distilled water and then in an aqueous solution of hematoxylin for staining for ~10 min at room temperature. After which, the slices were placed into ammonia and acid water for several sec, and then rinsed in running water for 1 h. The sections were placed in distilled water for several sec, and after which, dehydrated in alcohol at concentrations of 90 and 70% for 10 min each. Subsequently, the sections were stained with eosin staining solution for 2-3 min at room temperature. After staining, the samples were dehydrated with 100% alcohol and placed in xylene. The sections were sealed and placed in an incubator for drying. Images were obtained and collected using a ZEISS LSM 880 Confocal Microscope (Carl Zeiss AG). Image J (version 1.43; National Institutes of Health) was used to analyze the images. The ratio of the intima-media thickness to the outer diameter was calculated as a percentage of the intima-media thickness (30-32). The areaext (AE) represented the areas surrounded by external elastic plates, while the areaint (AI) represented the areas surrounded by internal elastic plates. The pulmonary artery wall thickness (WT) was calculated as follows: (AE-AI)/AE x100.

Immunofluorescence. Paraffin sections of lung tissue from rats were obtained from the embedded samples. The 5-μm paraffin sections were heated at 60˚C oven for 1 h, dewaxed twice in xylene solutions for 15 min each and rehydrated in a descending alcohol series. Antigen retrieval was performed with sodium citrate buffer (cat. no. C1031; Beijing Solarbio Science & Technology Co., Ltd.) at 100˚C for 10 min. After which, the 5-μm sections were incubated with 0.5% Triton X-100 and 5% BSA (cat. no. A8850-5; Beijing Solarbio Science & Technology Co., Ltd.) for 30 min at room temperature. The samples were incubated with the following primary antibodies at 4˚C overnight: Ki-67 (cat. no. ab92742; 1:200; Abcam) and α-SMA (cat. no. BM0002; 1:100; Boster Biological Technology). After which, the samples were incubated the following secondary antibodies: CoraLite488-conjugated Goat Anti-Mouse IgG (H + L; cat. no. SA00013-1; 1:100; Proteintech Group, Inc.) and CoraLite594-conjugated Goat Anti-Rabbit IgG (H + L; cat. no. SA00013-4; 1:100; Proteintech Group, Inc.) for 1 h at 37˚C. Finally, the nuclei were stained with DAPI for 10 min at 37˚C. Images were visualized and captured using a Nikon fluorescence microscope (Zeiss AG).

Detection of interleukin expression by ELISA. The levels of IL-1β and IL-18 in rat serum were determined using a Rat IL-18 ELISA Kit (cat. no. EK0592; Boster Biological Technology) and a Rat IL-1β/IL1B ELISA Kit (cat. no. EK0393; Boster Biological Technology). Experiments were performed according to the manufacturer's instructions. The OD value was determined, a standard curve was drawn and the sample concentration was calculated.

Protein extraction and quantification. Pulmonary arteries were isolated from SD rats. PBS was added to the blank culture dish, and the isolated pulmonary artery tissue was spread out in the culture dish. The adventitia of the pulmonary artery tissue was scraped with forceps. The pulmonary artery tissue was cut with ophthalmic scissors to expose the intima. The tunica intima of the pulmonary artery tissue was scraped with curved forceps, and the tunica media of the pulmonary artery, termed pulmonary artery smooth muscle cells, were obtained. Pulmonary artery smooth muscle cells were added to the lysate, homogenized with a homogenizer, diluted in lysate and centrifuged (at 4˚C for 15 min at 10,464 x g). The supernatant was used for the subsequent analyses. Protein concentrations were determined using a BCA kit (cat. no. AR1189; Boster Biological Technology) and sample volumes were calculated. The SDS-PAGE loading buffer (cat. no. CW0027S; CoWin Biosciences) was added and the sample was denatured for 6-10 min at 100˚C. After cooling, the protein was stored at -80˚C.

Western blotting. Samples were loaded at 20 μg per lane and electrophoresed by 10% SDS-PAGE. After partitioning by gel electrophoresis, the proteins were transferred onto polyvinylidene difluoride membranes (MilliporeSigma). The membranes were blocked in 5% non-fat milk for 2 h at room temperature and incubated for ~7 h at 4˚C with primary antibodies, including anti-GSDMD antibody (cat. no. sc-81868; 1:1,000; Santa Cruz Biotechnology, Inc.), anti-proliferating cell nuclear antigen (PCNA) antibody (cat. no. 13110S; 1:1,000; Cell Signaling Technology, Inc.), anti-NLRP3 antibody (cat. no. ab263899; 1:1,000; Abcam), anti-caspase-1 antibody (cat. no. NB100-56565; 1:2,000; Novus Biologicals, LLC), anti-GAPDH antibody (cat. no. BM3876; 1:2,000; Boster Biological Technology) and anti-β-actin antibody (cat. no. BM5422; 1:2,000; Boster Biological Technology). Stable protein references were selected based on the molecular weight of the target proteins. GAPDH (molecular weight, 36 kDa) was selected as the reference for NLRP3 (118 kDa), caspase-1 (53 kDa) and GSDMD (45 kDa), and β-actin (molecular weight, 42 kDa) was selected as the reference for PCNA (molecular weight, 36 kDa). Furthermore, the membranes were incubated with the appropriate secondary antibodies: HRP Conjugated AffiniPure Goat Anti-rabbit IgG (cat. no. BA1054; 1:5,000; Boster Biological Technology) and HRP Conjugated AffiniPure Goat Anti-mouse IgG (cat. no. BA1050; 1:5,000; Boster Biological Technology) for ~1 h. Thereafter, the bands were visualized using the Chemiluminescent Substrate kit (cat. no. PE0010; Beijing Solarbio Science & Technology Co., Ltd.) combined with a Tanon 5200 (Tanon Science and Technology Co., Ltd.), and densitometry analysis was performed using Image J (version 1.43; National Institutes of Health).

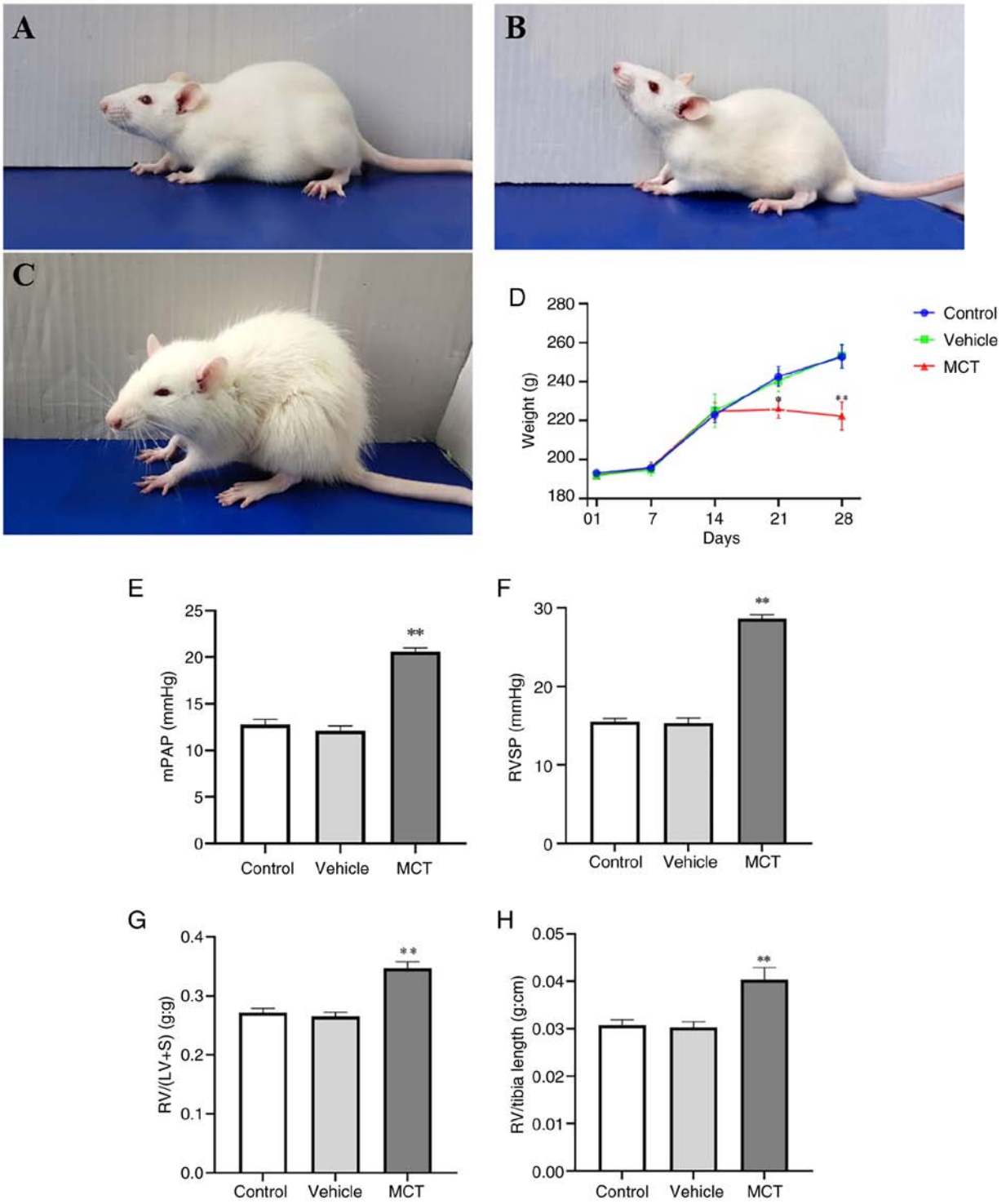

Figure 1. Hemodynamic changes and right ventricular remodeling in MCT-induced PAH rats. Images showing characteristics of (A) control rats, (B) vehicle rats and (C) MCT-induced PAH rats. (D) Weights of rats from the different groups. (E) mPAP. (F) RVSP. (G) Ratio of RV/(LV + S). (H) Ratio of RV weight to tibia length. Data are represented as the mean ± SEM (n=10). **P<0.01 vs. control group, and *P<0.05 vs. control group. MCT, monocrotaline; PAH, pulmonary arterial hypertension; mPAP, mean pulmonary artery pressure; RVSP, right ventricular systolic pressure; RV, right ventricle; LV, left ventricle; S, interventricular septum.

Statistical analysis. All data were analyzed using SPSS Statistics 21 (IBM Corp.) and graphics were generated using GraphPad Prism 8.0.2 (Dotmatics). Statistical values are expressed as the mean ± SEM and all experiments were repeated three times. One-way ANOVA with Tukey's post hoc test was used to compare multiple groups. P<0.05 was considered to indicate a statistically significant difference.

Results

Increased vascular remodeling and PASMC pyroptosis in MCT-induced PAH rats

Significant changes in characteristics of rats and hemodynamic changes. In the present study, a classical rat model of MCT-induced PAH was used to explore the specific mechanism

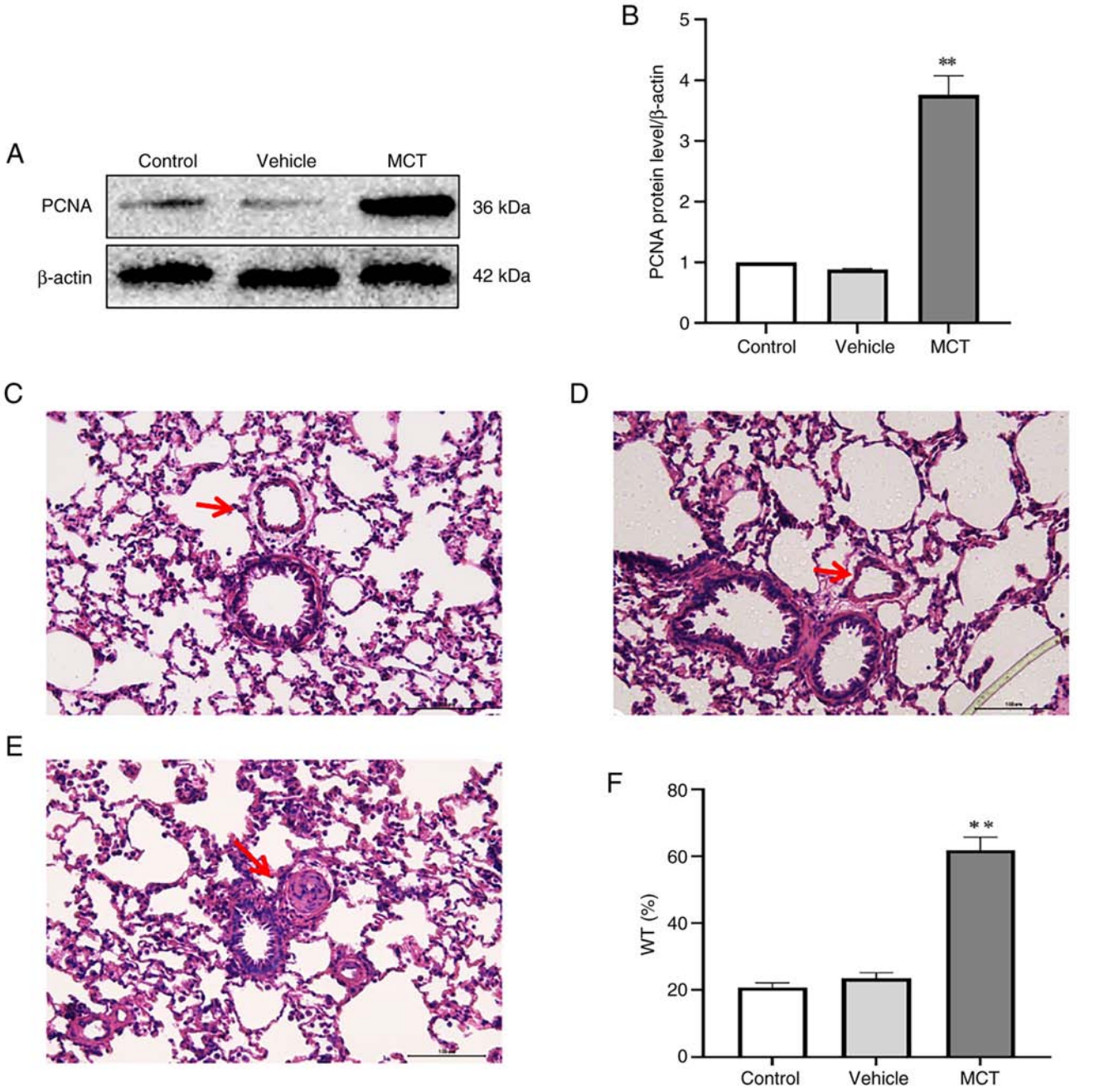

Figure 2. Pulmonary vascular remodeling was observed in MCT-induced PAH rats. (A) Western blotting and (B) quantification of the protein expression levels of PCNA from extracts of the lung tissue amongst the different groups. Pulmonary vascular remodeling was observed using HE staining in (C) control rats, (D) vehicle rats and (E) MCT rats (scale bar, 100 μm; magnification, 200x). The arrows show the pulmonary arterioles. (F) Quantitative analysis of the WT. Data are represented as the mean ± SEM (n=10), **P<0.01 vs. control group. MCT, monocrotaline; PAH, pulmonary arterial hypertension; PCNA, proliferating cell nuclear antigen; WT, pulmonary artery wall thickness.

of PASMC pyroptosis in pulmonary vascular remodeling. Compared with the control rats, MCT-treated rats showed notable mental distress, slow response, loss of appetite, rough hair, shortness of breath and emaciation (Fig. 1A-C). In addition, the weight of the MCT-induced rats significantly decreased during the final two weeks (Fig. 1D). To verify whether the modelling was successful, the hemodynamic changes in different groups were analyzed. The results demonstrated that RVSP, mPAP, RV/(LV + S) and RV weight/right tibial length were significantly higher in the MCT group than in the control group (P<0.01; Fig. 1E-H). Therefore, as aforementioned, the MCT-induced PAH rat model was successfully established.

Significant proliferation in PASMCs. Pulmonary artery smooth muscle cell proliferation obviously reflects the pulmonary vascular remodeling. The proliferation of PASMC was assessed by HE staining of lung tissues and PCNA protein expression. The results indicated that PCNA expression in PASMCs was significantly upregulated in the MCT group compared with the control group (Fig. 2A and B). It was found that the medial membrane of the pulmonary artery was thickened in the MCT group (Fig. 2C-E), and the percentage of WT in the MCT group was significantly higher than that in the control group (P<0.01; Fig. 2F). Furthermore, immunofluorescence showed that

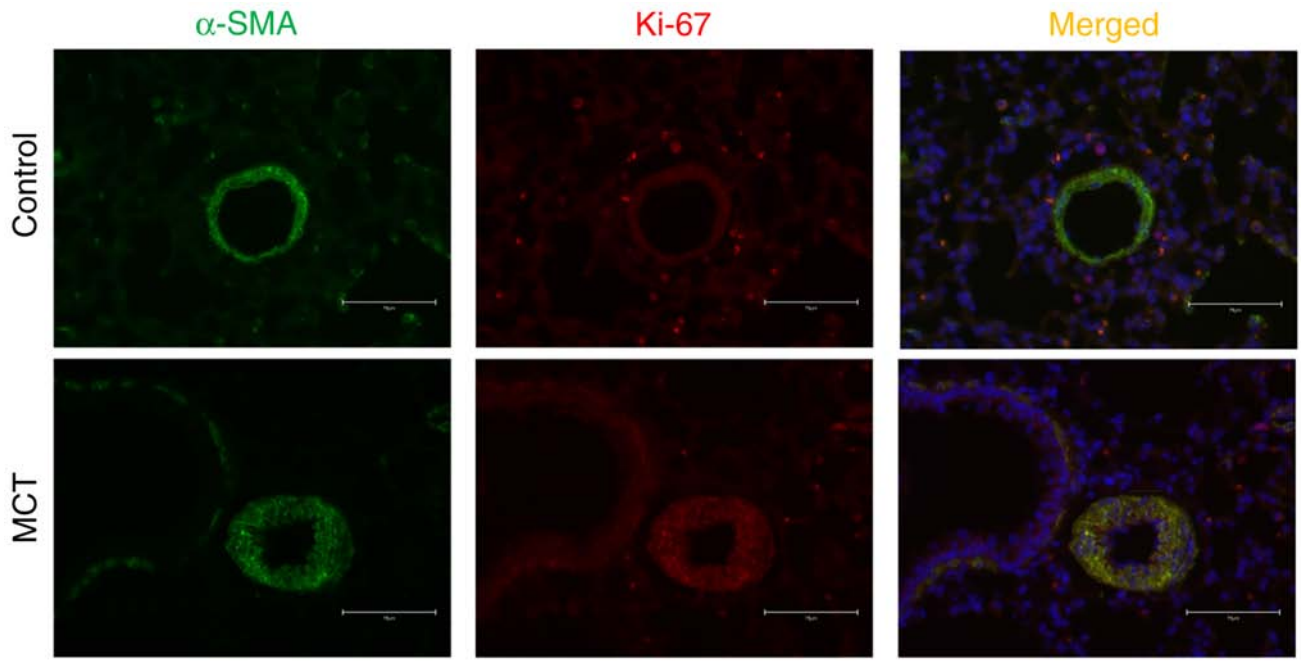

Figure 3. Increased expression of Ki-67 and pulmonary vascular remodeling were observed in MCT-induced PAH rats by immunofluorescence. Rats were treated with MCT or vehicle. The lung tissues were stained by immunofluorescence with α-SMA (α-smooth muscle actin) (green) used to label smooth muscle cells, and Ki-67 (red) used to reflect the degree of proliferation. Nuclei were stained with 4',6-diamidino-2-phenylindol (scale bar, 75 μm). MCT, monocrotaline; PAH, pulmonary arterial hypertension.

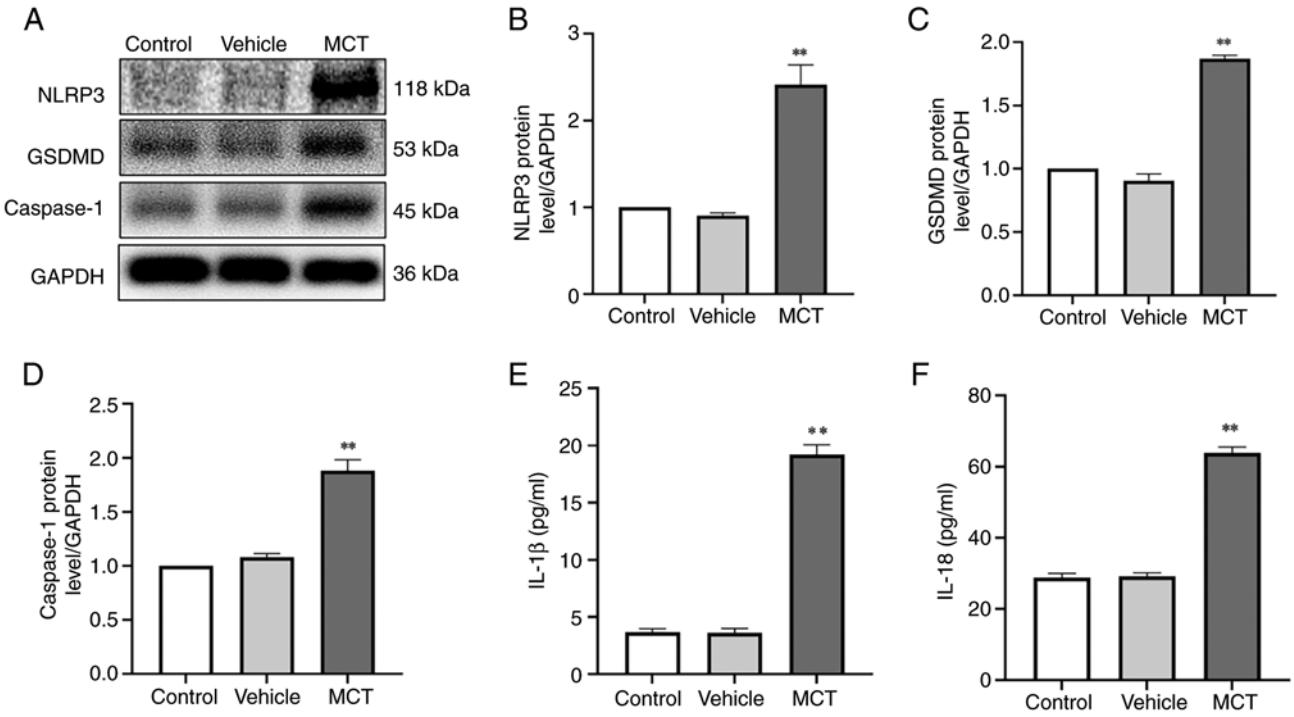

Figure 4. Increased pyroptosis of PASMCs, and IL-1β and IL-18 in MCT-induced PAH rats. (A) Western blotting and quantification of the protein expression levels of (B) NLRP3, (C) GSDMD and (D) caspase-1 from extracts of the lung tissue amongst the different groups. Levels of (E) IL-1β and (F) IL-18 were detected using ELISA. Data are represented as the mean ± SEM (n=10). **P<0.01 vs. control group. MCT, monocrotaline; PAH, pulmonary arterial hypertension; GSDMD, gasdermin D; NLRP3, Nod-like receptor protein 3.

the protein expression of Ki-67 in PASMCs in MCT-PAH rats was increased compared with that in the control rats (Fig. 3). These results indicated that PASMC proliferation increased after treatment with MCT (60 mg/kg) for 28 days. Based on these results, a rat model of MCT-induced PAH was successfully established. In addition, the vehicles had almost no impact on PASMC proliferation or pulmonary artery remodeling.

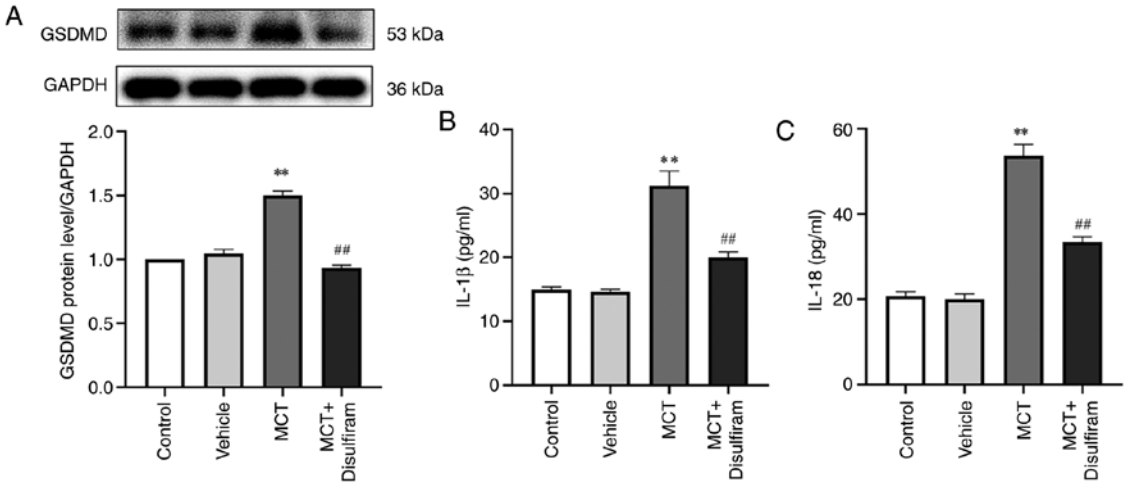

Figure 5. Disulfiram reverses the upregulation of GSDMD and inhibits IL-1β and IL-18 paracrine in MCT-induced PAH rats. (A) GSDMD expression was measured by western blotting. Levels of (B) IL-1β and (C) IL-18 were detected using ELISA. Data are represented as the mean ± SEM (n=10). **P<0.01 vs. control group and $^{\#\#}$P<0.01 vs. MCT group. MCT, monocrotaline; PAH, pulmonary arterial hypertension; GSDMD, gasdermin D.

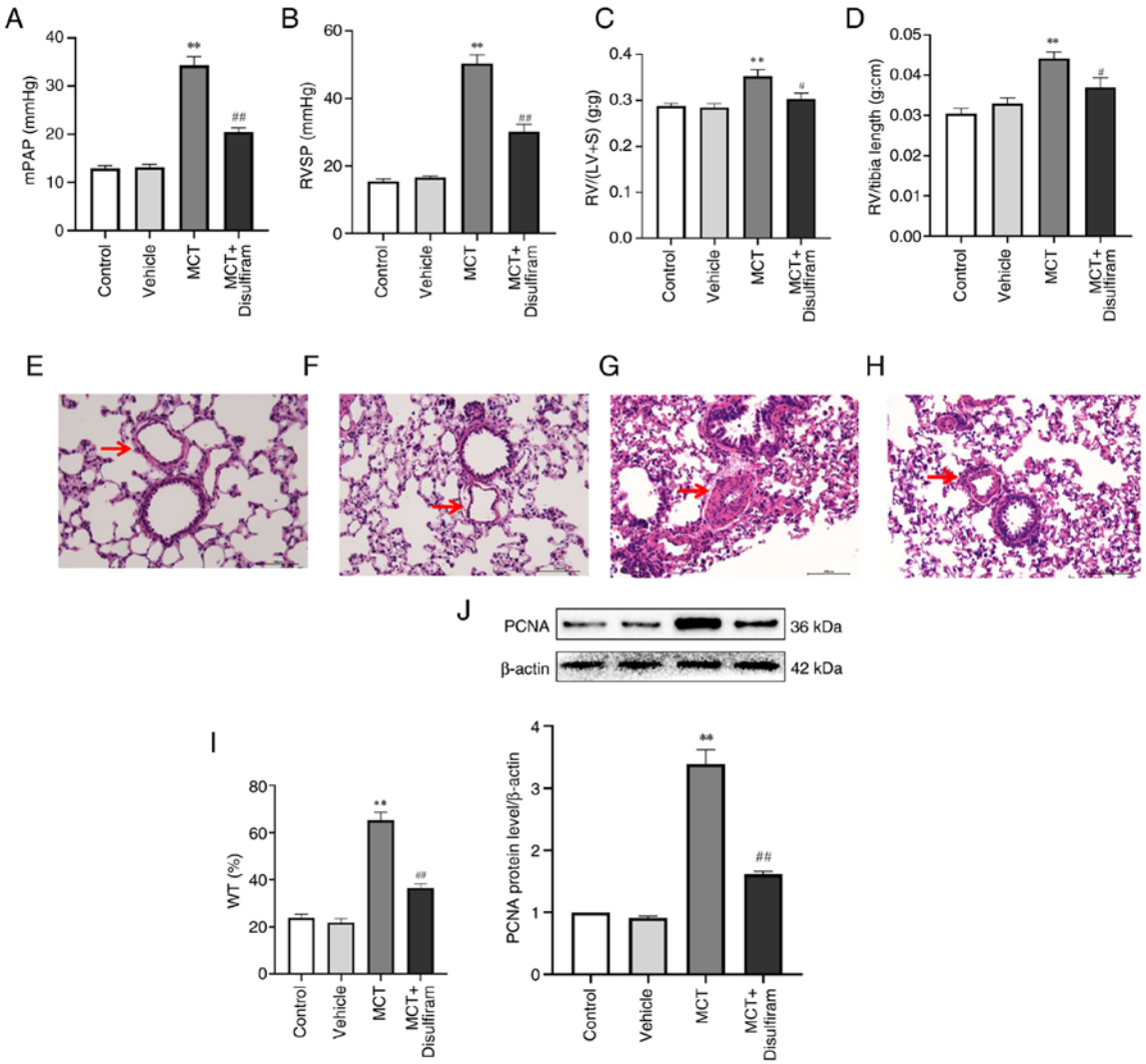

Figure 6. Inhibiting IL-1β and IL-18 paracrine attenuates PASMC proliferation and vascular remodeling in MCT-induced PAH rats. mPAP (A), RVSP (B), RV/(LV + S) (C) and RV/tibia length (D) in the disulfiram-induced rats were significantly decreased than those in the MCT-induced PAH rats. Pulmonary vascular remodeling was observed using HE staining in (E) control rats, (F) vehicle rats, (G) MCT rats and (H) MCT + disulfiram rats (scale bar, 100 μm; magnification, 200x). The arrows show the pulmonary arterioles. (I) Quantitative analysis of WT. (J) PCNA protein expression was measured by western blotting. Data are represented as the mean ± SEM (n=10) **P<0.01 vs. control group; $^{\#}$P<0.05, $^{\#\#}$P<0.01 vs. MCT group. MCT, monocrotaline; PAH, pulmonary arterial hypertension; mPAP, mean pulmonary artery pressure; RVSP, right ventricular systolic pressure; RV, right ventricle; LV, left ventricle; S, interventricular septum; WT, pulmonary artery wall thickness; PCNA, proliferating cell nuclear antigen; PASMC, pulmonary artery smooth muscle cell.

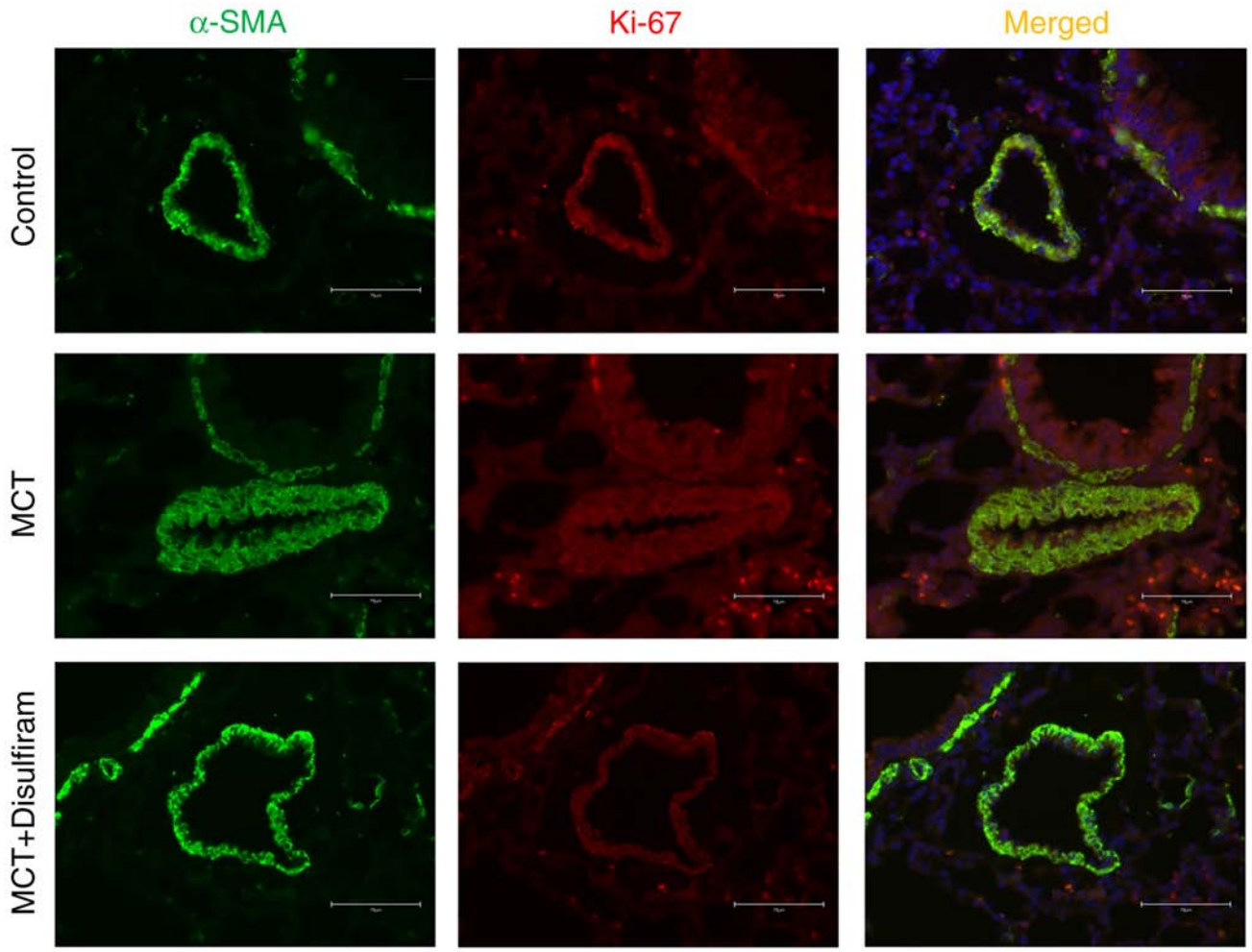

Figure 7. Pyroptosis inhibitor alleviates the expression of Ki-67 and pulmonary vascular remodeling in MCT-induced PAH rats. Rats were treated with MCT, MCT + disulfiram or vehicle. The lung tissues were stained by immunofluorescence with α-SMA (green) used to label smooth muscle cells and Ki-67 (red) used to reflect the degree of proliferation. Nuclei were stained with 4',6-diamidino-2-phenylindole (scale bar, 75 μm). MCT, monocrotaline; PAH, pulmonary arterial hypertension.

MCT induces PASMC pyroptosis. To determine whether PASMC pyroptosis is involved in the regulation of pulmonary vascular remodeling in MCT-induced PAH rats, the protein expression levels of NLRP3, GSDMD and caspase-1 were measured. As shown in Fig. 4, the protein expression levels of NLRP3, GSDMD and caspase-1 in PASMCs in the MCT group were significantly upregulated (P<0.01; Fig. 4A-D). These results indicated a significant increase in MCT-induced pyroptosis of PASMCs in rats with PAH.

PASMC pyroptosis promotes the proliferation of PASMCs via the paracrine effects of IL-1β and IL-18. To explore the regulatory mechanisms responsible for MCT-induced PASMC pyroptosis, the concentrations of interleukins were determined using ELISA. The levels of IL-1β and IL-18 in the MCT group were significantly higher than those in the control group (Fig. 4E and F). The results indicated that pyroptotic PASMCs could secrete IL-1β and IL-18. Therefore, PASMC pyroptosis may play a crucial role in promoting pulmonary vascular remodeling in MCT-induced PAH, and its molecular mechanism may be closely related to IL-1β and IL-18.

Disulfiram, a pyroptosis inhibitor, reverses the upregulation of GSDMD and inhibits the secretion of IL-1β and IL-18. To further clarify the important role of PASMC pyroptosis in pulmonary vascular remodeling and its molecular mechanisms, disulfiram, an inhibitor of GSDMD pore membrane and pyroptosis, was used to treat PAH rats. The present study revealed that GSDMD expression in disulfiram-treated PAH rats was significantly downregulated compared with that in MCT-induced rats (P<0.01; Fig. 5A). Increasing evidence suggests that IL-1β and IL-18 are involved in cell proliferation; however, it is unclear whether they influence PASMC proliferation in PAH. To determine the underlying mechanism through which PASMC pyroptosis indirectly promotes PASMC proliferation, the levels of interleukins in the serum of MCT-induced PAH rats were determined using ELISA. The results demonstrated that disulfiram lowers the concentrations of IL-1β and IL-18 in the serum of MCT-induced PAH rats (P<0.01; Fig. 5B and C). These results suggest that disulfiram can reduce the concentrations of IL-1β and IL-18 by inhibiting PASMC pyroptosis in MCT-induced PAH rats.

Inhibiting IL-1β and IL-18 paracrine signaling attenuates PASMC proliferation and vascular remodeling. To explore whether inhibiting IL-1β and IL-18 paracrine signaling can attenuate pulmonary artery remodeling, the hemodynamic

changes and the degree of cardiac and vascular remodeling in each group of rats were further compared. It was found that the RVSP, mPAP, RV/(LV + S) and RV weight/right tibia length in the disulfiram-treated PAH rats were significantly lower than those in the MCT-induced PAH rats (Fig. 6A-D). The aforementioned results revealed that inhibiting IL-1β and IL-18 paracrine signaling significantly attenuates right ventricular remodeling and inhibits pulmonary arterial thickening in MCT-induced PAH rats. To further prove that inhibiting IL-1β and IL-18 paracrine signaling attenuated PASMC hyperplasia, an inhibitory group model was established for comparative analysis. The results suggested that PCNA expression in PASMCs in the MCT-induced rats was significantly upregulated compared with that in the control rats. By contrast, it was significantly downregulated in the disulfiram-treated PAH rats compared with that in the MCT-induced rats (Fig. 6J). It was found that the pulmonary arterioles were significantly thicker in MCT-treated rats, and the percentage of WT was also significantly increased. Numerous inflammatory cells, such as lymphocytes and neutrophils, infiltrated the lung tissues of MCT-induced PAH rats. However, the opposite results were observed in disulfiram-treated PAH rats (Fig. 6E-I). In addition, it was found that disulfiram downregulated the protein expression of Ki-67 in PASMCs compared with that in MCT-induced PAH rats by immunofluorescence (Fig. 7). The aforementioned results suggest that inhibiting IL-1β and IL-18 paracrine signaling can attenuate PASMC proliferation and reverse vascular remodeling in MCT-induced PAH rats.

Discussion

PAH is a vascular disease characterized by pulmonary artery remodeling, increased afterload and cardiac hypertrophy (33). The proliferation of PASMCs significantly contributes to the occurrence and progression of PAH (11). The mechanism underlying pulmonary artery remodeling induced by PASMC proliferation has not yet been fully elucidated. Therefore, identifying new pathogenic and effective targets for PASMC proliferation is important for discovering preventative and early treatment therapies for PAH. The present study revealed the significant effect of PAMSC pyroptosis in PAH induced by MCT and clarifies that pyroptotic PASMCs can secrete IL-1β and IL-18, promote the proliferation of PASMCs and further facilitate pulmonary vascular remodeling. Furthermore, it was demonstrated that disulfiram can attenuate the progression of pulmonary hypertension, and the mechanisms may involve the secretion of IL-1β and IL-18.

Pyroptosis manifests as a form of pro-inflammatory cell death, accompanied by the formation of cell membrane pores and the secretion of various pro-inflammatory factors, especially the NLRP3 inflammasome and its downstream effector inflammatory factors IL-1β and IL-18 (15). Pyroptosis is widely associated with the progression of atherosclerosis, liver fibrosis, renal ischaemia/reperfusion injury and nervous system diseases (34-38). However, whether pyroptosis occurs in the PASMCs of MCT-induced PAH rats has not yet been reported. In the present study, it was found that pyroptosis significantly increased following MCT treatment in rats. Notably, PASMC pyroptosis was accompanied by the secretion of interleukins such as IL-1β and IL-18. GSDMD is a direct effector of pyroptosis and is an important target for the release of IL-1β and IL-18 (39). As aforementioned, PASMC pyroptosis may be crucial for MCT-induced pulmonary arterial remodeling. However, the regulatory mechanisms underlying the PASMC proliferation are unclear. Studies have indicated that the paracrine effects of IL-18 and IL-1β can promote human aortic smooth muscle cell migration and proliferation (40). Furthermore, a study on atherosclerotic mice showed that IL-1β can promote the proliferation, remodeling and structural maintenance of smooth muscle cells and fibrous caps (41). Importantly, reducing the level of IL-1β can inhibit smooth muscle cell proliferation and migration (42). Additionally, clinical studies have found that the levels of the interleukins IL-1β and IL-18 in the serum of patients with PAH are significantly increased (43-45). Pyroptosis of PASMCs is significantly increased in PAH rats, and interleukins play crucial roles in cardiovascular diseases. Thus, it would be useful to explore whether pyroptotic PASMCs can indirectly promote PASMC proliferation by secreting IL-18 and IL-1β.

The pore-forming activity of GSDMD directly determines the manner of death of cells, and GSDMD is the most direct and necessary executor of pyroptosis (46,47). The formation of membrane pores caused by GSDMD is a necessary step for the occurrence of pyroptosis. Disulfiram is a newly developed drug and Hu *et al* (48) found that disulfiram specifically inhibits the formation of the GSDMD pore membrane to prevent the secretion of inflammatory factors, and inhibit pyroptosis. IL-18 and IL-1β play important roles in cardiovascular disease (49,50). Notably, receptors for IL-1β and IL-18 are expressed at high levels on VSMCs (51,52). Moreover, high expression levels of IL-1β and IL-18 promote the proliferation and migration of VSMCs (53). To investigate whether pyroptosis can directly or indirectly promote PASMC proliferation and whether its mechanism is closely related to IL-1β and IL-18, disulfiram (a pyroptosis inhibitor) was used to explore its potential in reducing PASMC proliferation by inhibiting GSDMD pore formation and interleukin secretion. In the current study, it was confirmed that disulfiram can markedly downregulate the GSDMD protein expression and the concentrations of serum IL-1β and IL-18, reduce PASMC proliferation and reverse pulmonary vascular remodeling in PAH rats. Therefore, it is hypothesized that PASMC pyroptosis, a recently discovered mechanism of cell death, plays a vital role in promoting PASMC proliferation and facilitating pulmonary vascular remodeling. Notably, pyroptosis promotes PASMC proliferation and aggravates pulmonary vascular remodeling, possibly through paracrine IL-1β and IL-18.

PAH is a rare but fatal disease (1), and as the burden of PAH continues to increase, the prevention, treatment and research of PAH must be continuously strengthened. Increased pulmonary vascular resistance in PAH is driven by vasoconstriction, inflammation and proliferative remodeling of the intima and media of the pulmonary arteries (8). The strengths of the present study could be that experiments were carried out in an *in vivo* model and indicated a critical role for PASMC pyroptosis in MCT-induced PAH rats. In particular, an important strength could be that the experiments showed the crucial role of IL-1β and IL-18 in PASMC proliferation. The findings of the present study indicate that targeted inhibition of PASMC pyroptosis could effectively suppress PASMC proliferation

and relieve pulmonary vascular remodeling in PAH. It is also hypothesized that IL-1β and IL-18 could be used as novel targets for the prevention and treatment of PAH in the further research, and blocking the secretion of IL-1β and IL-18 may reduce and delay the development of PAH and improve the therapeutic effect of PAH. Therefore, this research could provide a new preventive and therapeutic strategy for PAH.

However, the present study had several limitations that must be addressed further. Firstly, the study confirmed that pyroptosis in PASMCs promotes their proliferation through the secretion of inflammatory factors *in vivo*. However, its role and mechanism of action have not been verified *in vitro*. At present, the primary culture of PASMCs is being performed with the intention of providing further evidence to reveal the effect of IL-1β and IL-18 on PASMC proliferation. In addition, a stain that specifically and targeted PASMC cells and their proliferation was not used in the present study. Moreover, the lack of female rats could be a limitation of the present study as estrogen may play a unique pathogenic or protective role in pulmonary hypertension (54,55). Male rats were used in the present study for a variety of reasons, such as to reduce variability due to hormonal differences between males and females, or to avoid potential complications related to the estrous cycle in female animals. IN addition, at present, researcher investigating the pathogenesis of PAH have exclusively used male SD rats (56-58). Finally, further studies with greater samples are required.

In conclusion, the present study confirmed the new pathogenesis of MCT-induced PAH in rats. Pyroptosis of PASMCs plays an important role in MCT-induced PAH in rats. PASMC pyroptosis is significantly increased in PAH rats and can markedly promote PASMC proliferation, possibly by secreting IL-1β and IL-18, which could be useful for identifying novel therapeutic strategies against PASMC pyroptosis to reverse PAH. Targeting the inhibition of GSDMD pore membrane formation can markedly reduce the concentrations of IL-1β and IL-18, inhibit PASMC proliferation and further reverse pulmonary artery remodeling in MCT-induced PAH rats. The present study demonstrated the crucial role and mechanism of PASMC pyroptosis in pulmonary artery remodeling and provided an important basis for developing new therapeutic strategies for PAH. Blocking the pyroptosis of PVSMCs provides a novel therapeutic strategy of PAH. With the advancing of related research and the improvement of detection technology, treatment of anti-PASMC pyroptosis has potential. In the future, exploring the inhibition of pyroptosis and their intrinsic mechanisms, will make significance contributions to the discovery of novel therapeutic targets and the development of new drugs for PAH.

Acknowledgements

Not applicable.

Funding

This project was supported by The National Natural Science Foundation of China (grant no. 81600040), The Natural Science Foundation of the Province of Hunan (grant no. 2021JJ30601), Key Program of Education Department of Hunan Province (grant no. 21A0274), Key Guidance Program of Health Commission of Hunan Province (grant no. 20201905), The Clinical Medical Research Center of Hunan (grant no. 2020SK4007) and Hunan Provincial Health High-Level Talent Scientific Research Project (grant no. R2023068).

Availability of data and materials

The data generated in the present study may be requested from the corresponding author.

Authors' contributions

APW, XFM and YT conceived and designed the experiments and obtained the funding. QYZ and WL wrote the article. QYZ, APW and XFM revised the manuscript. QYZ and WL completed the ELISA and western blotting experiments.QYZ, WL, APW, YT and XFM analyzed all the data. SXG performed the HE staining. QYZ and WL conducted animal experiments. YT, XFM and APW supervised the project. APW and XFM confirm the authenticity of all the raw data. All authors read and approved the final version of the manuscript.

Ethics approval and consent to participate

All animal experiments were performed in strict accordance with the ARRIVE guidelines and were approved by The Animal Ethics Committee of the University of South China (Hengyang, China; approval no. 446).

Patient consent for publication

Not applicable

Competing interests

The authors declare that they have no competing interests.

References

1. Breault NM, Wu D, Dasgupta A, Chen KH and Archer SL: Acquired disorders of mitochondrial metabolism and dynamics in pulmonary arterial hypertension. Front Cell Dev Biol 11:1105565, 2023.
2. Galiè N, McLaughlin VV, Rubin LJ and Simonneau G: An overview of the 6th world symposium on pulmonary hypertension. Eur Respir J 53: 1802148, 2019.
3. Van Nuffel S, Quatredeniers M, Pirkl A, Zakel J, Le Caer JP, Elie N, Vanbellingen QP, Dumas SJ, Nakhleh MK, Ghigna MR, *et al*: Multimodal imaging mass spectrometry to identify markers of pulmonary arterial hypertension in human lung tissue using MALDI-ToF, ToF-SIMS, and hybrid SIMS. Anal Chem 92: 12079-12087, 2020.
4. Samokhin AO, Hsu S, Yu PB, Waxman AB, Alba GA, Wertheim BM, Hopkins CD, Bowman F, Channick RN, Nikolic I, *et al*: Circulating NEDD9 is increased in pulmonary arterial hypertension: A multicenter, retrospective analysis. J Heart Lung Transplant 39: 289-299, 2020.
5. Guignabert C, Savale L, Boucly A, Thuillet R, Tu L, Ottaviani M, Rhodes CJ, De Groote P, Prévot G, Bergot E, *et al*: Serum and pulmonary expression profiles of the activin signaling system in pulmonary arterial hypertension. Circulation 147: 1809-1822, 2023.
6. Tang H, Desai AA and Yuan JX: Genetic insights into pulmonary arterial hypertension. application of whole-exome sequencing to the study of pathogenic mechanisms. Am J Respir Crit Care Med 194: 393-397, 2016.

7. Frid MG, McKeon BA, Thurman JM, Maron BA, Li M, Zhang H, Kumar S, Sullivan T, Laskowsky J, Fini MA, *et al*: Immunoglobulin-driven complement activation regulates proinflammatory remodeling in pulmonary hypertension. Am J Respir Crit Care Med 201: 224-239, 2020.
8. Yun X, Philip NM, Jiang H, Smith Z, Huetsch JC, Damarla M, Suresh K and Shimoda LA: Upregulation of aquaporin 1 mediates increased migration and proliferation in pulmonary vascular cells from the rat SU5416/hypoxia model of pulmonary hypertension. Front Physiol 12: 763444, 2021.
9. Luo L, Hong X, Diao B, Chen S and Hei M: Sulfur dioxide attenuates hypoxia- induced pulmonary arteriolar remodeling via Dkk1/Wnt signaling pathway. Biomed Pharmacother 106: 692-698, 2018.
10. Jia D, He Y, Zhu Q, Liu H, Zuo C, Chen G, Yu Y and Lu A: RAGE-mediated extracellular matrix proteins accumulation exacerbates HySu-induced pulmonary hypertension. Cardiovasc Res 113: 586-597, 2017.
11. Dean A, Gregorc T, Docherty CK, Harvey KY, Nilsen M, Morrell NW and MacLean MR: Role of the aryl hydrocarbon receptor in sugen 5416-induced experimental pulmonary hypertension. Am J Respir Cell Mol Biol 58: 320-330, 2018.
12. Parpaleix A, Amsellem V, Houssaini A, Abid S, Breau M, Marcos E, Sawaki D, Delcroix M, Quarck R, Maillard A, *et al*: Role of interleukin-1 receptor 1/MyD88 signalling in the development and progression of pulmonary hypertension. Eur Respir J 48: 470-483, 2016.
13. Zehendner CM, Valasarajan C, Werner A, Boeckel JN, Bischoff FC, John D, Weirick T, Glaser SF, Rossbach O, Jaé N, *et al*: Long noncoding RNA TYKRIL plays a role in pulmonary hypertension via the p53-mediated regulation of PDGFRβ. Am J Respir Crit Care Med 202: 1445-1457, 2020.
14. Wang AP, Yang F, Tian Y, Su JH, Gu Q, Chen W, Gong SX, Ma XF, Qin XP and Jiang ZS: Pulmonary artery smooth muscle cell senescence promotes the proliferation of PASMCs by paracrine IL-6 in hypoxia-induced pulmonary hypertension. Front Physiol 12: 656139, 2021.
15. Zhaolin Z, Guohua L, Shiyuan W and Zuo W: Role of pyroptosis in cardiovascular disease. Cell Prolif 52: e12563, 2019.
16. Duan H, Zhang X, Song R, Liu T, Zhang Y and Yu A: Upregulation of miR-133a by adiponectin inhibits pyroptosis pathway and rescues acute aortic dissection. Acta Biochim Biophys Sin (Shanghai) 52: 988-997, 2020.
17. Gong T, Yang Y, Jin T, Jiang W and Zhou R: Orchestration of NLRP3 inflammasome activation by ion fluxes. Trends Immunol 39: 393-406, 2018.
18. Banerjee I, Behl B, Mendonca M, Shrivastava G, Russo AJ, Menoret A, Ghosh A, Vella AT, Vanaja SK, Sarkar SN, *et al*: Gasdermin D restrains type I interferon response to cytosolic DNA by disrupting ionic homeostasis. Immunity 49: 413-426. e5, 2018.
19. Liu X, Zhang Z, Ruan J, Pan Y, Magupalli VG, Wu H and Lieberman J: Inflammasome-activated gasdermin D causes pyroptosis by forming membrane pores. Nature 535: 153-158, 2016.
20. Xu YJ, Zheng L, Hu YW and Wang Q: Pyroptosis and its relationship to atherosclerosis. Clin Chim Acta 476: 28-37, 2018.
21. Pan J, Han L, Guo J, Wang X, Liu D, Tian J, Zhang M and An F: AIM2 accelerates the atherosclerotic plaque progressions in ApoE-/- mice. Biochem Biophys Res Commun 498: 487-494, 2018.
22. Pan J, Lu L, Wang X, Liu D, Tian J, Liu H, Zhang M, Xu F and An F: AIM2 regulates vascular smooth muscle cell migration in atherosclerosis. Biochem Biophys Res Commun 497: 401-409, 2018.
23. Cheng KT, Xiong S, Ye Z, Hong Z, Di A, Tsang KM, Gao X, An S, Mittal M, Vogel SM, *et al*: Caspase-11-mediated endothelial pyroptosis underlies endotoxemia-induced lung injury. J Clin Invest 127: 4124-4135, 2017.
24. Zhaolin Z, Jiaojiao C, Peng W, Yami L, Tingting Z, Jun T, Shiyuan W, Jinyan X, Dangheng W, Zhisheng J and Zuo W: OxLDL induces vascular endothelial cell pyroptosis through miR-125a-5p/TET2 pathway. J Cell Physiol 234: 7475-7491, 2019.
25. Li P, Dong XR, Zhang B, Zhang XT, Liu JZ, Ma DS and Ma L: Molecular mechanism and therapeutic targeting of necrosis, apoptosis, pyroptosis, and autophagy in cardiovascular disease. Chin Med J (Engl) 134: 2647-2655, 2021.
26. Wilson DW, Segall HJ, Pan LC, Lamé MW, Estep JE and Morin D: Mechanisms and pathology of monocrotaline pulmonary toxicity. Crit Rev Toxicol 22: 307-325, 1992.
27. Kovacs SB and Miao EA: Gasdermins: Effectors of pyroptosis. Trends Cell Biol 27: 673-684, 2017.
28. Wang L, Li K, Lin X, Yao Z, Wang S, Xiong X, Ning Z, Wang J, Xu X, Jiang Y, *et al*: Metformin induces human esophageal carcinoma cell pyroptosis by targeting the miR-497/PELP1 axis. Cancer Lett 450: 22-31, 2019.
29. McKenzie BA, Mamik MK, Saito LB, Boghozian R, Monaco MC, Major EO, Lu JQ, Branton WG and Power C: Caspase-1 inhibition prevents glial inflammasome activation and pyroptosis in models of multiple sclerosis. Proc Natl Acad Sci USA 115: E6065-E6074, 2018.
30. Wang AP, Li XH, Gong SX, Li WQ, Hu CP, Zhang Z and Li YJ: miR-100 suppresses mTOR signaling in hypoxia-induced pulmonary hypertension in rats. Eur J Pharmacol 765: 565-573, 2015.
31. Guo L, Li Y, Tian Y, Gong S, Chen X, Peng T, Wang A and Jiang Z: eIF2α promotes vascular remodeling via autophagy in monocrotaline-induced pulmonary arterial hypertension rats. Drug Des Devel Ther 13: 2799-2809, 2019.
32. Liu B, Peng Y, Yi D, Machireddy N, Dong D, Ramirez K, Dai J, Vanderpool R, Zhu MM, Dai Z and Zhao YY: Endothelial PHD2 deficiency induces nitrative stress via suppression of caveolin-1 in pulmonary hypertension. Eur Respir J 60: 2102643, 2022.
33. Sharifi Kia D, Kim K and Simon MA: Current understanding of the right ventricle structure and function in pulmonary arterial hypertension. Front Physiol 12: 641310, 2021.
34. Wei Y, Lan B, Zheng T, Yang L, Zhang X, Cheng L, Tuerhongjiang G, Yuan Z and Wu Y: GSDME-mediated pyroptosis promotes the progression and associated inflammation of atherosclerosis. Nat Commun 14: 929, 2023.
35. Yang F, Qin Y, Wang Y, Li A, Lv J, Sun X, Che H, Han T, Meng S, Bai Y and Wang L: LncRNA KCNQ1OT1 mediates pyroptosis in diabetic cardiomyopathy. Cell Physiol Biochem 50: 1230-1244, 2018.
36. Tonnus W, Maremonti F, Belavgeni A, Latk M, Kusunoki Y, Brucker A, von Mässenhausen A, Meyer C, Locke S, Gembardt F, *et al*: Gasdermin D-deficient mice are hypersensitive to acute kidney injury. Cell Death Dis 13: 792, 2022.
37. Gaul S, Leszczynska A, Alegre F, Kaufmann B, Johnson CD, Adams LA, Wree A, Damm G, Seehofer D, Calvente CJ, *et al*: Hepatocyte pyroptosis and release of inflammasome particles induce stellate cell activation and liver fibrosis. J Hepatol 74: 156-167, 2021.
38. Moonen S, Koper MJ, Van Schoor E, Schaeverbeke JM, Vandenberghe R, von Arnim CAF, Tousseyn T, De Strooper B and Thal DR: Pyroptosis in Alzheimer's disease: Cell type-specific activation in microglia, astrocytes and neurons. Acta Neuropathol 145: 175-195, 2023.
39. Dai R, Ren Y, Lv X, Chang C, He S, Li Q, Yang X, Ren L, Wei R and Su Q: MicroRNA-30e-3p reduces coronary microembolism-induced cardiomyocyte pyroptosis and inflammation by sequestering HDAC2 from the *SMAD7* promoter. Am J Physiol Cell Physiol 324: C222-C235, 2023.
40. Sukhanov S, Higashi Y, Yoshida T, Mummidi S, Aroor AR, Jeffrey Russell J, Bender SB, DeMarco VG and Chandrasekar B: The SGLT2 inhibitor empagliflozin attenuates interleukin-17A-induced human aortic smooth muscle cell proliferation and migration by targeting TRAF3IP2/ROS/NLRP3/Caspase-1-dependent IL-1β and IL-18 secretion. Cell Signal 77: 109825, 2021.
41. Gomez D, Baylis RA, Durgin BG, Newman AAC, Alencar GF, Mahan S, St Hilaire C, Müller W, Waisman A, Francis SE, *et al*: Interleukin-1β has atheroprotective effects in advanced atherosclerotic lesions of mice. Nat Med 24: 1418-1429, 2018.
42. Haldar S, Dru C, Choudhury D, Mishra R, Fernandez A, Biondi S, Liu Z, Shimada K, Arditi M and Bhowmick NA: Inflammation and pyroptosis mediate muscle expansion in an interleukin-1β (IL-1β)-dependent manner. J Biol Chem 290: 6574-6583, 2015.
43. Saito T, Miyagawa K, Chen SY, Tamosiuniene R, Wang L, Sharpe O, Samayoa E, Harada D, Moonen JAJ, Cao A, *et al*: Upregulation of human endogenous retrovirus-K is linked to immunity and inflammation in pulmonary arterial hypertension. Circulation 136: 1920-1935, 2017.
44. Mavrogiannis E, Hagdorn QAJ, Bazioti V, Douwes JM, Van Der Feen DE, Oberdorf-Maass SU, Westerterp M and Berger RMF: Pirfenidone ameliorates pulmonary arterial pressure and neointimal remodeling in experimental pulmonary arterial hypertension by suppressing NLRP3 inflammasome activation. Pulm Circ 12: e12101, 2022.
45. Choudhury P, Dasgupta S, Kar A, Sarkar S, Chakraborty P, Bhattacharyya P, Roychowdhury S and Chaudhury K: Bioinformatics analysis of hypoxia associated genes and inflammatory cytokine profiling in COPD-PH. Respir Med 227: 107658, 2024.

46. Chen X, He WT, Hu L, Li J, Fang Y, Wang X, Xu X, Wang Z, Huang K and Han J: Pyroptosis is driven by non-selective gasdermin-D pore and its morphology is different from MLKL channel-mediated necroptosis. Cell Res 26: 1007-1020, 2016.
47. Ding J, Wang K, Liu W, She Y, Sun Q, Shi J, Sun H, Wang DC and Shao F: Pore-forming activity and structural autoinhibition of the gasdermin family. Nature 535:111-116, 2016.
48. Hu JJ, Liu X, Xia S, Zhang Z, Zhang Y, Zhao J, Ruan J, Luo X, Lou X, Bai Y, *et al*: FDA-approved disulfiram inhibits pyroptosis by blocking gasdermin D pore formation. Nat Immunol 21: 736-745, 2020.
49. Liu S, Deng X, Zhang P, Wang X, Fan Y, Zhou S, Mu S, Mehta JL and Ding Z: Blood flow patterns regulate PCSK9 secretion via MyD88-mediated pro-inflammatory cytokines. Cardiovasc Res 116: 1721-1732, 2020.
50. Westphal E, Herzberg M, Neumann I, Beibei L, Pilowski C, Li C, Werdan K and Loppnow H: Neutrophils process interleukin-1beta and interleukin-18 precursors in a caspase-1-like fashion-processing is inhibited by human vascular smooth muscle cells. Eur Cytokine Netw 17: 19-28, 2006.
51. Porritt RA, Zemmour D, Abe M, Lee Y, Narayanan M, Carvalho TT, Gomez AC, Martinon D, Santiskulvong C, Fishbein MC, *et al*: NLRP3 inflammasome mediates immune-stromal interactions in vasculitis. Circ Res 129: e183-e200, 2021.
52. Sahar S, Dwarakanath RS, Reddy MA, Lanting L, Todorov I and Natarajan R: Angiotensin II enhances interleukin-18 mediated inflammatory gene expression in vascular smooth muscle cells: A novel cross-talk in the pathogenesis of atherosclerosis. Circ Res 96: 1064-1071, 2005.
53. Li P, Li YL, Li ZY, Wu YN, Zhang CC, A X, Wang CX, Shi HT, Hui MZ, Xie B, *et al*: Cross talk between vascular smooth muscle cells and monocytes through interleukin-1β/interleukin-18 signaling promotes vein graft thickening. Arterioscler Thromb Vasc Biol 34: 2001-2011, 2014.
54. Rodriguez-Arias JJ and García-Álvarez A: Sex differences in pulmonary hypertension. Front Aging 2: 727558, 2021.
55. Sun Y, Sangam S, Guo Q, Wang J, Tang H, Black SM and Desai AA: Sex differences, estrogen metabolism and signaling in the development of pulmonary arterial hypertension. Front Cardiovasc Med 8: 719058, 2021.
56. Huang Y, Lei C, Xie W, Yan L, Wang Y, Yuan S, Wang J, Zhao Y, Wang Z, Yang X, *et al*: Oxidation of ryanodine receptors promotes Ca2+ leakage and contributes to right ventricular dysfunction in pulmonary hypertension. Hypertension 77: 59-71, 2021.
57. Yan X, Huang J, Zeng Y, Zhong X, Fu Y, Xiao H, Wang X, Lian H, Luo H, Li D and Guo R: CGRP attenuates pulmonary vascular remodeling by inhibiting the cGAS-STING-NFκB pathway in pulmonary arterial hypertension. Biochem Pharmacol 222: 116093, 2024.
58. Williams TL, Nyimanu D, Kuc RE, Foster R, Glen RC, Maguire JJ and Davenport AP: The biased apelin receptor agonist, MM07, reverses sugen/hypoxia-induced pulmonary arterial hypertension as effectively as the endothelin antagonist macitentan. Front Pharmacol 15: 1369489, 2024.